

The triple Higgs coupling: A new probe of low-scale seesaw models

Julien Baglio, Cédric Weiland

Institute for Theoretical Physics, University of Tübingen, Auf der Morgenstelle 14, 72076 Tübingen, Germany

Institute for Particle Physics Phenomenology, Department of Physics, Durham University, South Road, Durham DH1 3LE, United Kingdom

E-mail: julien.baglio@uni-tuebingen.de, cedric.weiland@durham.ac.uk

ABSTRACT: The measure of the triple Higgs coupling is one of the major goals of the high-luminosity run of the CERN Large Hadron Collider (HL-LHC) as well as the future colliders, either leptonic such as the International Linear Collider (ILC) or hadronic such as the 100 TeV Future Circular Collider in hadron-hadron mode (FCC-hh). We have recently proposed this observable as a test of neutrino mass generating mechanisms in a regime where heavy sterile neutrino masses are hard to be probed otherwise. We present in this article a study of the one-loop corrected triple Higgs coupling in the inverse seesaw model, taking into account all relevant constraints on the model. This is the first study of the impact on the triple Higgs coupling of heavy neutrinos in a realistic, renormalizable neutrino mass model. We obtain deviations from the Standard Model as large as to $\sim +30\%$ that are at the current limit of the HL-LHC sensitivity, but would be clearly visible at the ILC or at the FCC-hh.

KEYWORDS: Beyond Standard Model, Neutrino Physics, Higgs Physics

Contents

1	Introduction	1
2	Model and constraints	2
2.1	The inverse seesaw model	3
2.2	Constraints on the ISS model	5
3	Framework of the calculation	7
4	Numerical results	9
4.1	Casas-Ibarra parameterization	10
4.2	Degenerate heavy neutrinos	12
4.3	Hierarchical heavy neutrinos	14
5	Conclusions	16
A	Next order corrections to the μ_X-parameterization	17
B	Analytic expressions of the new ISS contributions	18
B.1	Counter-terms	19
B.2	One-loop un-renormalized self energy Σ_{HH} and vertex $\lambda_{HHH}^{(1)}$	19

1 Introduction

The CERN Large Hadron Collider (LHC) was home to one of the biggest discoveries in particle physics with the observation of a Higgs boson with a mass of around 125 GeV in 2012 [1, 2], thanks to the data collected in Run 1 at 7 and 8 TeV. The Higgs boson is the remnant of the electroweak symmetry-breaking (EWSB) mechanism [3–6] that generates the masses of the other fundamental particles and unitarizes the scattering of weak bosons [7, 8]. The Run 2 data collected in 2015 and 2016 at a center-of-mass energy of 13 TeV still displays a compatibility of this Higgs boson with the Standard Model (SM) hypothesis; nevertheless we know that the SM cannot be the ultimate theory. In particular the observation of neutrino oscillations, confirmed in 1998 at Super-Kamiokande [9], implies that neutrinos are massive, which cannot be explained in the SM framework and thus calls for an extension of the SM. One of the simplest possibilities to explain the non-zero neutrino masses and mixing is to add fermionic gauge singlets that will play the role of right-handed neutrinos. The addition of these heavy sterile neutrinos leads to the type I seesaw model and its various extensions [10–25].

In a recent article [26] we have presented the triple Higgs coupling λ_{HHH} as a new observable to test neutrino mass generating mechanisms in a regime of mass difficult to probe otherwise. The measure of λ_{HHH} is one of the main goals of the high-luminosity run of the LHC (HL-LHC) as well as of the future colliders, such as the electron-positron International Linear Collider (ILC) [27] or the Future Circular Collider in hadron-hadron mode (FCC-hh), a potential 100 TeV pp collider (for the Higgs studies see reviews in refs. [28–30]). It would be a direct probe of the shape of the scalar potential that triggers EWSB. Any deviation of this coupling from the SM prediction is then welcomed to unravel new physics. In ref. [26] the study of neutrino effects on λ_{HHH} was done in the context of a simplified model with the SM plus one heavy Dirac neutrino. It was found that effects as large as +30% at one-loop could be obtained, at the limit of the currently foreseen $\sim 35\%$ sensitivity that the HL-LHC will have to the SM triple Higgs coupling, when combining ATLAS and CMS data [31], but clearly measurable at the ILC [32] or the FCC [33]. A comprehensive study in a realistic and renormalizable model of neutrino masses was still left to be done.

In this article, we fill the gap and present the first analysis of Majorana neutrino effects on λ_{HHH} . We work within the inverse seesaw (ISS) model [17–19], a renormalizable low-scale seesaw model generating neutrino masses. After taking into account all relevant constraints, we obtain effects that can be as large as a $\sim +30\%$ increase of λ_{HHH} , similar to the effects that we found in our previous article [26] using a simplified model. In the case of the ISS model, more heavy neutrinos are present, enhancing the effects as we expected, but the constraints on the model are stronger, reducing the end-effect back to the simplified model expectations. This can be clearly measurable at the ILC and at the FCC-hh and is at the limit of the currently foreseen sensitivity of the HL-LHC.

This article is organized as follows. In Section 2 we present the ISS model as well as the theoretical and experimental constraints that we consider. We give the technical details of our calculation in Section 3 and present the numerical analysis of the ISS one-loop corrections to λ_{HHH} in Section 4. A short conclusion is given in Section 5. We present the details of the parameterization adopted for the light neutrino mass matrix in Appendix A and the analytical expressions of the one-loop corrections involving the neutrinos are collected in Appendix B.

2 Model and constraints

While our calculation and the analytical results presented in Section 3 are applicable to all models with extra fermionic gauge singlets and Majorana neutrinos like the type I seesaw [10–16] or the linear seesaw [22–25], we will focus in this work on the inverse seesaw (ISS) model for illustrative purposes. After introducing the model and the different parameterizations used to reproduce neutrino oscillations data, we will present the theoretical and experimental constraints considered in our study.

2.1 The inverse seesaw model

One particular variant of the type 1 seesaw is the ISS model [17–19] which has very interesting characteristics leading to a rich phenomenology. In the ISS model the suppression mechanism that guarantees the smallness of neutrino masses is the introduction of a slight breaking of lepton number in the singlet sector (composed of right-handed neutrinos ν_R and new gauge singlets X with opposite lepton number), in the form of a small Majorana mass μ_X for the X singlets, compared to the electroweak scale $v \sim 246$ GeV. This allows for large Yukawa couplings compatible with a low (TeV or even lower) mass for the seesaw mediators, contrary to the seesaw model of type I for example, where the mediators have a mass of the order of the GUT scale or the Yukawa couplings are very small.

In the inverse seesaw, the additional terms to the SM Lagrangian are

$$\mathcal{L}_{\text{ISS}} = -Y_\nu^{ij} \bar{L}_i \tilde{\Phi} \nu_{Rj} - M_R^{ij} \bar{\nu}_{Ri}^C X_j - \frac{1}{2} \mu_X^{ij} \bar{X}_i^C X_j + h.c., \quad (2.1)$$

where Φ is the Higgs field and $\tilde{\Phi} = i\sigma_2 \Phi^*$, $i, j = 1 \dots 3$, Y_ν and M_R are complex matrices and μ_X is a complex symmetric matrix whose norm is taken to be small since lepton number is assumed to be nearly conserved. In this work, we do not consider a possible Majorana mass term for the right-handed neutrinos ν_R since this extra parameter is not relevant to our study. It would only induce negligible corrections to the heavy neutrino masses and the observable that we consider conserves lepton number. Assuming 3 pairs of ν_R and X , the 9×9 neutrino mass matrix reads after electroweak symmetry breaking in the basis (ν_L^C, ν_R, X) ,

$$M_{\text{ISS}} = \begin{pmatrix} 0 & m_D & 0 \\ m_D^T & 0 & M_R \\ 0 & M_R^T & \mu_X \end{pmatrix}, \quad (2.2)$$

with the 3×3 Dirac mass matrix given by $m_D = Y_\nu \langle \Phi \rangle$. M_{ISS} being complex and symmetric, we can use the Takagi factorization to write

$$U_\nu^T M_{\text{ISS}} U_\nu = \text{diag}(m_{n_1}, \dots, m_{n_9}), \quad (2.3)$$

where U_ν is a 9×9 unitary matrix.

A specificity of the ISS model is the presence of a nearly conserved lepton number. The light neutrino masses are then suppressed by the small lepton number breaking parameter μ_X and the heavy Majorana neutrinos, which have nearly degenerate masses, form pseudo-Dirac pairs. This can clearly be seen if we consider only one generation. In the inverse seesaw limit $\mu_X \ll m_D, M_R$, we have one light neutrino ν and two heavy neutrinos N_1, N_2 with masses

$$m_\nu \simeq \frac{m_D^2}{m_D^2 + M_R^2} \mu_X, \quad (2.4)$$

$$m_{N_1, N_2} \simeq \sqrt{M_R^2 + m_D^2} \mp \frac{M_R^2 \mu_X}{2(m_D^2 + M_R^2)}. \quad (2.5)$$

With three generations, M_{ISS} can be diagonalized by block to give the light neutrino mass matrix, at leading order in the seesaw expansion parameter $m_D M_R^{-1}$,

$$M_{\text{light}} \simeq m_D M_R^{T-1} \mu_X M_R^{-1} m_D^T. \quad (2.6)$$

The next order terms are given in Appendix A. This 3×3 mass matrix is diagonalized by using the unitary Pontecorvo-Maki-Nakagawa-Sakata (PMNS) matrix U_{PMNS} [34, 35]:

$$U_{\text{PMNS}}^T M_{\text{light}} U_{\text{PMNS}} = \text{diag}(m_{n_1}, m_{n_2}, m_{n_3}) \equiv m_\nu, \quad (2.7)$$

with m_{n_1} , m_{n_2} and m_{n_3} the masses of the three light neutrinos.

In order to reproduce low-energy neutrino data, different parameterizations can be introduced. Working in the basis where M_R is diagonal with entries M_i , neutrino oscillations are generated by off-diagonal terms in m_D and μ_X . In a first parameterization, we can reconstruct m_D as a function of neutrino oscillation data and high energy parameters. This leads to a Casas-Ibarra parameterization [36] adapted to the inverse seesaw

$$m_D^T = V^\dagger \text{diag}(\sqrt{M_1}, \sqrt{M_2}, \sqrt{M_3}) R \text{diag}(\sqrt{m_{n_1}}, \sqrt{m_{n_2}}, \sqrt{m_{n_3}}) U_{\text{PMNS}}^\dagger, \quad (2.8)$$

where M_1, M_2, M_3 are the positive square roots of $M M^\dagger$ and M is defined by

$$M = M_R \mu_X^{-1} M_R^T. \quad (2.9)$$

V is a unitary matrix that diagonalize M according to $M = V^\dagger \text{diag}(M_1, M_2, M_3) V^*$ and R is a complex orthogonal matrix that can be expressed as

$$R = \begin{pmatrix} c_2 c_3 & -c_1 s_3 - s_1 s_2 c_3 & s_1 s_3 - c_1 s_2 c_3 \\ c_2 s_3 & c_1 c_3 - s_1 s_2 s_3 & -s_1 c_3 - c_1 s_2 s_3 \\ s_2 & s_1 c_2 & c_1 c_2 \end{pmatrix}, \quad (2.10)$$

with $c_i = \cos \theta_i$, $s_i = \sin \theta_i$, θ_i being arbitrary complex angles.

The other possibility is to use the μ_X -parameterization that was introduced in [37], giving

$$\mu_X = M_R^T m_D^{-1} U_{\text{PMNS}}^* m_\nu U_{\text{PMNS}}^\dagger m_D^{T-1} M_R. \quad (2.11)$$

Both parameterizations are based on eq.(2.6) where only the leading order term in the seesaw expansion is considered. While this is sufficient in most of the parameter space, these formulas fail to reproduce low-energy neutrino data when the active-sterile mixing becomes very large. Including the next order terms in the seesaw expansion in the μ_X -parameterization gives

$$\begin{aligned} \mu_X \simeq & \left(\mathbf{1} - \frac{1}{2} M_R^{*-1} m_D^\dagger m_D M_R^{T-1} \right)^{-1} M_R^T m_D^{-1} U_{\text{PMNS}}^* m_\nu U_{\text{PMNS}}^\dagger m_D^{T-1} M_R \times \\ & \left(\mathbf{1} - \frac{1}{2} M_R^{-1} m_D^T m_D^* M_R^{\dagger-1} \right)^{-1}, \end{aligned} \quad (2.12)$$

which allows to better reproduce neutrino oscillation data. The complete derivation of this formula is given in Appendix A.

Finally, we need to specify the couplings between SM particles and the new fields that are relevant for our calculation of the corrections to the triple Higgs coupling λ_{HHH} . Following [21], we introduce the B and C matrices defined as

$$B_{ij} = \sum_{k=1}^3 V_{L\,ki}^* U_{\nu\,kj}^*, \quad (2.13)$$

$$C_{ij} = \sum_{k=1}^3 U_{\nu\,ki} U_{\nu\,kj}^*, \quad (2.14)$$

where V_L is the unitary matrix that diagonalizes the charged lepton mass matrix M_{charged} according to

$$V_L^\dagger M_{\text{charged}} V_R = \text{diag}(m_e, m_\mu, m_\tau), \quad (2.15)$$

with V_R another unitary matrix. In the Feynman-'t Hooft gauge and in the mass basis, the relevant interaction terms in the Lagrangian are

$$\begin{aligned} \mathcal{L}_{\text{int}}^Z &= -\frac{g_2}{4 \cos \theta_W} \bar{n}_i \not{Z} [C_{ij} P_L - C_{ij}^* P_R] n_j, \\ \mathcal{L}_{\text{int}}^H &= -\frac{g_2}{4m_W} H \bar{n}_i [(C_{ij} m_{n_i} + C_{ij}^* m_{n_j}) P_L + (C_{ij} m_{n_j} + C_{ij}^* m_{n_i}) P_R] n_j, \\ \mathcal{L}_{\text{int}}^{G^0} &= \frac{ig_2}{4m_W} G^0 \bar{n}_i [-(C_{ij} m_{n_i} + C_{ij}^* m_{n_j}) P_L + (C_{ij} m_{n_j} + C_{ij}^* m_{n_i}) P_R] n_j, \\ \mathcal{L}_{\text{int}}^{W^\pm} &= -\frac{g_2}{\sqrt{2}} \bar{l}_i B_{ij} \not{W}^\pm P_L n_j + h.c., \\ \mathcal{L}_{\text{int}}^{G^\pm} &= \frac{-g_2}{\sqrt{2}m_W} G^\pm [\bar{l}_i B_{ij} (m_{l_i} P_L - m_{n_j} P_R) n_j] + h.c., \end{aligned} \quad (2.16)$$

where g_2 is the SU(2) coupling constant, θ_W is the weak mixing angle and P_L, P_R are respectively $(1 - \gamma_5)/2$ and $(1 + \gamma_5)/2$.

2.2 Constraints on the ISS model

Strong experimental and theoretical constraints on the parameter space of the model have to be considered, in particular on the size of the active-sterile mixing. Our use of the modified Casas-Ibarra or μ_X -parameterization allows to reproduce neutrino oscillation data. In our numerical study, we explicitly check the agreement with the neutrino masses and mixing obtained in the global fit NuFIT 3.0 [38]. The light neutrino masses are also chosen to agree with the Planck result [39]

$$\sum_{i=1}^3 m_{n_i} < 0.23 \text{ eV}. \quad (2.17)$$

The mixing between the active and sterile neutrinos will also induce deviations from unitarity in the 3×3 sub-matrix \tilde{U}_{PMNS} of the full 9×9 mixing matrix U_ν , that controls the mixing

between the light neutrinos. Using a polar decomposition, this square complex matrix can be expressed as

$$\tilde{U}_{\text{PMNS}} = (I - \eta) U_{\text{PMNS}}, \quad (2.18)$$

where η is a Hermitian matrix that encodes the deviations from unitarity. We have included the following constraints from a recent fit [40] to electroweak precision observables, tests of CKM unitarity and tests of lepton universality,

$$\begin{aligned} \sqrt{2|\eta_{ee}|} &< 0.050, & \sqrt{2|\eta_{e\mu}|} &< 0.026, \\ \sqrt{2|\eta_{\mu\mu}|} &< 0.021, & \sqrt{2|\eta_{e\tau}|} &< 0.052, \\ \sqrt{2|\eta_{\tau\tau}|} &< 0.075, & \sqrt{2|\eta_{\mu\tau}|} &< 0.035. \end{aligned} \quad (2.19)$$

In the presence of a large active-sterile mixing, the off-diagonal entries in the neutrino Yukawa couplings Y_ν might also induce large branching ratios for lepton flavor violating (LFV) decays. We have implemented the analytical expressions from [21] for the LFV radiative decays and the LFV three-body decays. The corresponding experimental upper limits on the LFV radiative decays [41, 42] are

$$\text{Br}(\mu^+ \rightarrow e^+ \gamma) < 4.2 \times 10^{-13}, \quad (2.20)$$

$$\text{Br}(\tau^\pm \rightarrow e^\pm \gamma) < 3.3 \times 10^{-8}, \quad (2.21)$$

$$\text{Br}(\tau^\pm \rightarrow \mu^\pm \gamma) < 4.4 \times 10^{-8}, \quad (2.22)$$

at 90% C.L. while the upper limits on LFV three-body decays [43, 44] are

$$\text{Br}(\mu^+ \rightarrow e^+ e^+ e^-) < 1.0 \times 10^{-12}, \quad (2.23)$$

$$\text{Br}(\tau^- \rightarrow e^- e^+ e^-) < 2.7 \times 10^{-8}, \quad (2.24)$$

$$\text{Br}(\tau^- \rightarrow \mu^- \mu^+ \mu^-) < 2.1 \times 10^{-8}, \quad (2.25)$$

$$\text{Br}(\tau^- \rightarrow e^- \mu^+ \mu^-) < 2.7 \times 10^{-8}, \quad (2.26)$$

$$\text{Br}(\tau^- \rightarrow \mu^- e^+ e^-) < 1.8 \times 10^{-8}, \quad (2.27)$$

$$\text{Br}(\tau^- \rightarrow e^+ \mu^- \mu^-) < 1.7 \times 10^{-8}, \quad (2.28)$$

$$\text{Br}(\tau^- \rightarrow \mu^+ e^- e^-) < 1.5 \times 10^{-8}, \quad (2.29)$$

at 90% C.L.

We will also require in our study that Yukawa couplings are perturbative since the complex angles of the R matrix in the Casas-Ibarra parameterization or the use of Y_ν as an input parameter in the μ_X -parameterization can lead to arbitrarily large entries in Y_ν . We will ensure the perturbativity of the Yukawa couplings by requiring

$$\frac{|Y_{ij}|^2}{4\pi} < 1.5, \quad (2.30)$$

for $i, j = 1 \dots 3$. Since the decay width of heavy neutrinos grows like m_n^3 when $m_n \gg m_H$, we also requires that their decay width verifies, for $i = 4 \dots 9$,

$$\Gamma_{n_i} < 0.6 m_{n_i}, \quad (2.31)$$

in order for the quantum state to be a definite particle. The formulae used to calculate the heavy neutrino widths are taken from Ref. [45].

3 Framework of the calculation

Our calculation is done in the Feynman-'t Hooft gauge and we use the Lagrangian of eq.(2.16) for the neutrino interactions. The SM scalar potential is written as

$$V(\Phi) = -\mu^2 |\Phi|^2 + \lambda |\Phi|^4, \quad (3.1)$$

with the Higgs field Φ given by

$$\Phi = \frac{1}{\sqrt{2}} \begin{pmatrix} \sqrt{2} G^+ \\ v + H + i G^0 \end{pmatrix}. \quad (3.2)$$

H stands for the Higgs boson, G^0 the neutral Goldstone boson, G^\pm the charged Goldstone bosons and $v \simeq 246$ GeV is the vacuum expectation value (vev) of the Higgs field. We can define the Higgs tadpole t_H , the Higgs mass M_H and the triple Higgs coupling λ_{HHH} as follows,

$$\begin{aligned} t_H &= - \left\langle \frac{\partial V}{\partial H} \right\rangle, \\ M_H^2 &= \left\langle \frac{\partial^2 V}{\partial H^2} \right\rangle, \\ \lambda_{HHH} &= - \left\langle \frac{\partial^3 V}{\partial H^3} \right\rangle. \end{aligned} \quad (3.3)$$

This helps to redefine the triple Higgs coupling using t_H , M_H and v as input parameters,

$$\lambda_{HHH} = - \frac{3M_H^2}{v} \left(1 + \frac{t_H}{vM_H^2} \right). \quad (3.4)$$

At tree-level, $t_H = 0$ and we recover the usual definition of the tree-level triple Higgs coupling,

$$\lambda^0 = - \frac{3M_H^2}{v}. \quad (3.5)$$

For the one-loop corrections to the triple Higgs coupling, our set of input parameters that need to be renormalized in the on-shell (OS) scheme will be the following:

$$M_H, M_W, M_Z, e, t_H. \quad (3.6)$$

We use the following relations to define the Higgs vev v and the weak angle θ_W ,

$$\begin{aligned} v &= 2 \frac{M_W \sin \theta_W}{e}, \\ \sin^2 \theta_W &= 1 - \frac{M_W^2}{M_Z^2}, \end{aligned} \quad (3.7)$$

as well as $e^2 = 4\pi\alpha$.

We require that we have no tadpoles at one loop:

$$t_H^{(1)} + \delta t_H = 0 \Rightarrow \delta t_H = -t_H^{(1)}, \quad (3.8)$$

with $t_H^{(1)}$ being the one-loop un-renormalized contributions to t_H . For the other parameters we introduce their counter-terms as follows,

$$\begin{aligned} M_H^2 &\rightarrow M_H^2 + \delta M_H^2, \\ M_W^2 &\rightarrow M_W^2 + \delta M_W^2, \\ M_Z^2 &\rightarrow M_Z^2 + \delta M_Z^2, \\ e &\rightarrow (1 + \delta Z_e) e, \\ H &\rightarrow \sqrt{Z_H} H = \left(1 + \frac{1}{2} \delta Z_H\right) H. \end{aligned} \quad (3.9)$$

The full renormalized one-loop triple Higgs coupling is finally

$$\lambda_{HHH}^{1r}(q_H^*) = \lambda^0 + \lambda_{HHH}^{(1)}(q_H^*) + \delta \lambda_{HHH}, \quad (3.10)$$

with

$$\begin{aligned} \delta \lambda_{HHH} &= \lambda^0 \left[\frac{3}{2} \delta Z_H + \delta t_H \frac{e}{2 M_W \sin \theta_W M_H^2} + \delta Z_e + \frac{\delta M_H^2}{M_H^2} - \frac{\delta M_W^2}{2 M_W^2} \right. \\ &\quad \left. + \frac{1}{2} \frac{\cos^2 \theta_W}{\sin^2 \theta_W} \left(\frac{\delta M_W^2}{M_W^2} - \frac{\delta M_Z^2}{M_Z^2} \right) \right], \end{aligned} \quad (3.11)$$

and $\lambda_{HHH}^{(1)}(q_H^*)$ stands for the un-renormalized one-loop contributions to the process $H^* \rightarrow HH$ with the momentum q_H^* for the off-shell Higgs boson H^* . For the numerical analysis carried in the next section, we define the deviation induced by the BSM contribution Δ^{BSM} as

$$\Delta^{\text{BSM}} = \frac{1}{\lambda_{HHH}^{1r, \text{SM}}} \left(\lambda_{HHH}^{1r} - \lambda_{HHH}^{1r, \text{SM}} \right), \quad (3.12)$$

where $\lambda_{HHH}^{1r, \text{SM}}$ stands for the renormalized one-loop SM contribution without the light neutrinos.

Introducing the notation Σ_{XY} for the self-energy of the process $X \rightarrow Y$, we use the usual OS conditions for M_W , M_Z and M_H ,

$$\begin{aligned}\delta M_W^2 &= \text{Re } \Sigma_{WW}^T(M_H^2), \\ \delta M_Z^2 &= \text{Re } \Sigma_{ZZ}^T(M_H^2), \\ \delta M_H^2 &= \text{Re } \Sigma_{HH}(M_H^2).\end{aligned}\tag{3.13}$$

For the electric charge e we use the following condition to be independent from the light fermion masses [46, 47],

$$\delta Z_e = \frac{\sin \theta_W}{\cos \theta_W} \frac{\text{Re } \Sigma_{\gamma Z}^T(0)}{M_Z^2} - \frac{\text{Re } \Sigma_{\gamma\gamma}^T(M_Z^2)}{M_Z^2}.\tag{3.14}$$

For the Higgs field renormalization we have

$$\delta Z_H = -\text{Re} \left. \frac{\partial \Sigma_{HH}(k^2)}{\partial k^2} \right|_{k^2=M_H^2}.\tag{3.15}$$

The neutrino interactions induce changes in the W and Z self-energies as well as in the Higgs tadpole, self-energy and self-couplings. We display in Fig. 1 the Feynman diagrams for the neutrino contributions to the W , Z and Higgs bosons self-energies, the Higgs tadpole and the one-loop un-renormalized triple Higgs coupling. We also collect in Appendix B the analytical expressions of the neutrino contributions to δM_W , δM_Z , δt_H , Σ_{HH} and $\lambda_{HHH}^{(1)}$. They were obtained using `FeynArts` 2.7 [48] and `FormCalc` 7.5 [49], in which we have implemented our own Model File for the ISS model. The scalar and tensor loop functions [50, 51] have been evaluated with `LoopTools` 2.13 [49, 52, 53]. We have checked numerically that the UV divergences cancel in the final result and that the renormalized one-loop triple Higgs coupling does not depend on the choice of the renormalization scale.

4 Numerical results

We present in this section the phenomenological study of the one-loop corrected triple Higgs coupling and the dependence of the corrections induced by the heavy neutrinos on the relevant input parameters of the ISS model. The SM parameters are taken from the Particle Data Group (PDG) [54] (with the exception of the SM Higgs boson mass) and read as

$$\begin{aligned}m_t^{\text{pole}} &= 173.5 \text{ GeV}, & m_b^{\text{pole}} &= 4.77 \text{ GeV}, & m_c^{\text{pole}} &= 1.42 \text{ GeV}, \\ M_W &= 80.385 \text{ GeV}, & M_Z &= 91.1876 \text{ GeV}, & M_H &= 125 \text{ GeV}, \\ m_e &= 0.511 \text{ MeV}, & m_\mu &= 105.7 \text{ MeV}, & m_\tau &= 1.777 \text{ GeV}, \\ \alpha^{-1}(M_Z^2) &= 127.934.\end{aligned}\tag{4.1}$$

The up-, down- and strange-quark masses are also taken from the PDG, but their impact on the calculation is negligible so that we do not list them here. The lightest neutrino mass

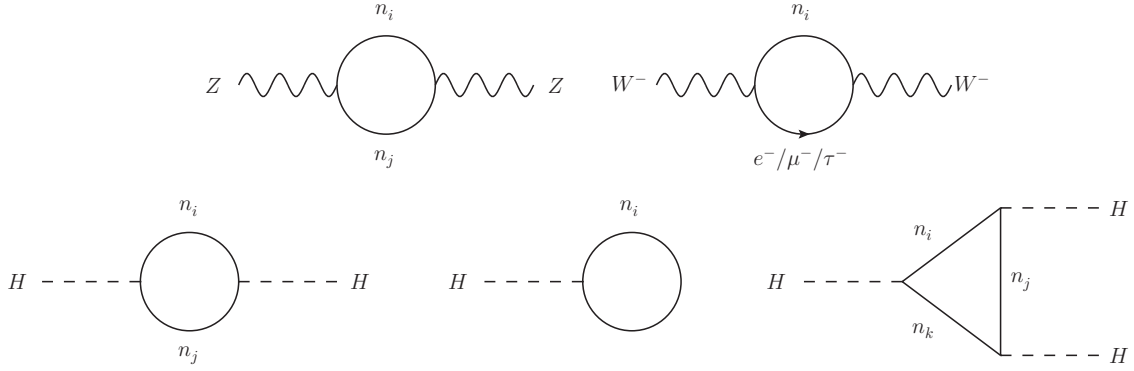


Figure 1. Feynman diagrams for the neutrino contributions to the one-loop W and Z boson self-energies (upper line) and the one-loop Higgs boson self energy, tadpole and triple Higgs coupling (lower line). In all diagrams, the indices $i/j/k$ run from 1 to 9.

is chosen as

$$m_{n_1} = 0.01 \text{ eV}, \quad (4.2)$$

to comply with cosmological constraints as stated in eq.(2.17). We chose the normal ordering for the neutrino masses and the light neutrino mixing parameters are taken from NuFIT 3.0 [38], with $\delta_{\text{CP}} = 0$. Since the contributions of the light neutrinos are negligible and flavor constraints do not play an important role in our final conclusion, we do not expect our conclusion to change if we consider the inverted ordering.

4.1 Casas-Ibarra parameterization

In order to get an insight into the parameter space of the ISS model we perform a scan in a Casas-Ibarra parameterization, see eq.(2.8). The goal is to get an idea of the corrections that are obtained in this parameterization and the impact of the constraints on the model. We perform a random scan using a flat prior on the three real rotation angles $\theta_{1/2/3}$ of the orthogonal matrix R and a logarithmic prior on both the lepton number violating term μ_X so that the Majorana mass term is $\mu_X \equiv \mu_X \mathbf{I}_3$, and the mass term M_R so that the matrix M_R is $M_R \equiv M_R \mathbf{I}_3$. We do not consider CP violation so that all mixing masses and rotation matrices are taken real.

We use 180 000 randomly generated points in the following parameter range,

$$\begin{aligned} 0 &\leq \theta_i \leq 2\pi, \quad (i = 1 \dots 3), \\ 0.2 \text{ TeV} &\leq M_R \leq 1000 \text{ TeV}, \\ 7.00 \times 10^{-4} \text{ eV} &\leq \mu_X \leq 8.26 \times 10^4 \text{ eV}. \end{aligned} \quad (4.3)$$

The range choice for the parameter μ_X follows $\mu_X^{\text{min}[\text{max}]} = \left(M_R^{\text{min}[\text{max}]}\right)^2 \frac{m_{n_1}}{3\pi v^2 [2v^2]}$, see eq.(2.4).

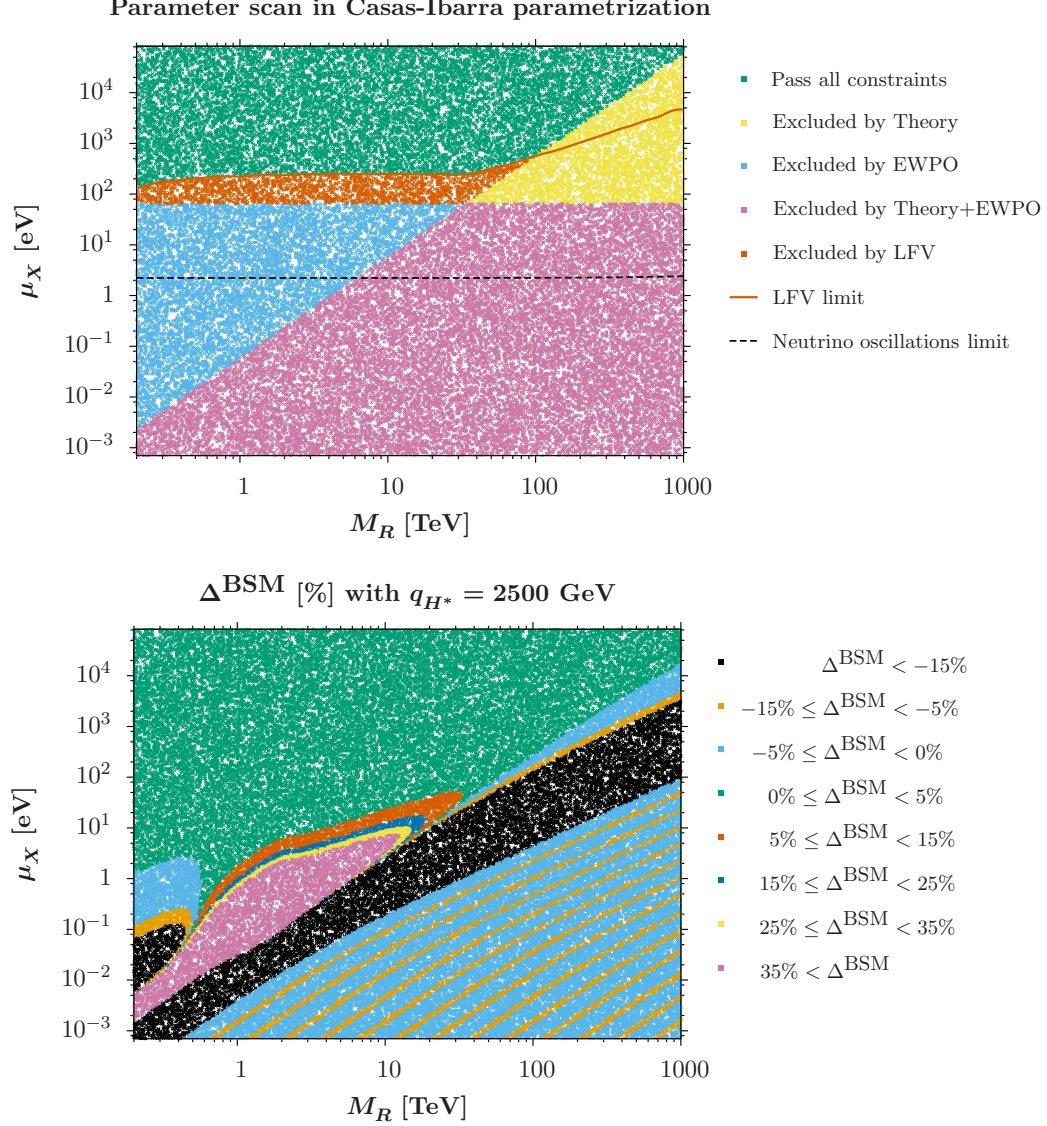


Figure 2. Random scan of the parameter space with 180 000 points in the Casas-Ibarra parametrization as a function of M_R (in TeV) and of μ_X (in eV). Left: Map of the points according to the constraints on the model. The vermilion (solid) line stands for the LFV constraints and the black (dashed) line stands for the constraints coming from neutrino oscillations. All points below these lines are excluded. In green, the points that pass all the constraints; in yellow, the points that are excluded by theory constraints; in blue, the points that are excluded by EWPO; in purple, the points that are excluded both by EWPO and theory constraints. Right: Map of Δ^{BSM} correction (in percent). In black: $\Delta^{\text{BSM}} < -15\%$; in orange: $-15\% \leq \Delta^{\text{BSM}} < -5\%$; in light blue: $-5\% \leq \Delta^{\text{BSM}} < 0\%$; in green: $0\% \leq \Delta^{\text{BSM}} < 5\%$; in vermilion: $5\% \leq \Delta^{\text{BSM}} < 15\%$; in blue: $15\% \leq \Delta^{\text{BSM}} < 25\%$; in yellow: $25\% \leq \Delta^{\text{BSM}} < 35\%$; in purple: $\Delta^{\text{BSM}} > 35\%$.

The result of our scan is displayed in Fig. 2 (left) in the $M_R - \mu_X$ plane. The top-right corner (in yellow) of the parameter space is excluded by theory constraints, essentially the perturbativity of the neutrino Yukawa couplings. The region in light blue is excluded by EWPO, while the region in purple is excluded both by EWPO and theory constraints. The dashed black line displays the limit coming from neutrino oscillations. This comes from a breakdown of the leading-order Casas-Ibarra parameterization when the active-sterile mixing is too large, as is evidenced by the flat behavior in M_R . Indeed in the Casas-Ibarra parameterization, the active-sterile mixing is independent from M_R , in a first approximation, and this limit roughly corresponds to $m_D/M_R \geq 0.5$. The most stringent experimental constraint comes from LFV observables as displayed by the solid vermilion line. The top-left corner (in green) is allowed by all the constraints.

This scan has to be compared to the map of Δ^{BSM} displayed in Fig. 2 (right), fixing the off-shell Higgs momentum at $q_H^* = 2500$ GeV. The parameter space passing all the constraints only contains corrections up to $\sim +1\%$. The most interesting regions are in vermilion, blue, yellow and purple where Δ^{BSM} reaches $+15\%$, $+25\%$, $+35\%$ and more than $+35\%$, respectively. In order to enter these regions, it is needed to escape the LFV constraints as much as possible. Following Ref. [37] we will investigate this region using the μ_X -parameterization and start with the case of degenerate heavy neutrinos.

4.2 Degenerate heavy neutrinos

The scan in the Casas-Ibarra parameterization displayed in Fig. 2 shows that the most stringent constraints come from LFV observables. In order to maximize the effects on the triple Higgs coupling we want to escape these constraints and we require for example $(Y_\nu Y_\nu^\dagger)_{12} = 0$ since decays that involve a $\mu - e$ transition usually give the strongest constraints. This leads to either a diagonal Yukawa matrix or a Yukawa texture as defined in ref. [37], with degenerate heavy neutrinos, $M_R \propto \mathbb{I}_3$.

We investigate in this sub-section the case of the degenerate heavy neutrinos in a μ_X -parameterization with the texture $Y_{\tau\mu}^{(1)}$ taken from ref. [37] and defined below,

$$Y_{\tau\mu}^{(1)} = |Y_\nu| \begin{pmatrix} 0 & 1 & -1 \\ 0.9 & 1 & 1 \\ 1 & 1 & 1 \end{pmatrix}. \quad (4.4)$$

We display in Fig. 3 (left) the two-dimensional scan in the plane $(M_R, |Y_\nu|)$ where M_R represents the common scaling factor of the 3×3 diagonal mass matrix M_R . The off-shell Higgs momentum is again fixed at $q_H^* = 2500$ GeV. A large part of the parameter space is excluded and a maximum of $\Delta^{\text{BSM}} \sim +5\%$ can be reached at $M_R \simeq 13$ TeV. When compared to the Casas-Ibarra scan, this is the expected order of magnitude for the correction when entering the vermilion region which is excluded by LFV observables only. For large M_R the most important constraint is the neutrino width (2.31). For lower M_R the constraints are driven by the violation of the unitarity of the 3×3 matrix \tilde{U}_{PMNS} controlling the mixing between the light neutrinos.

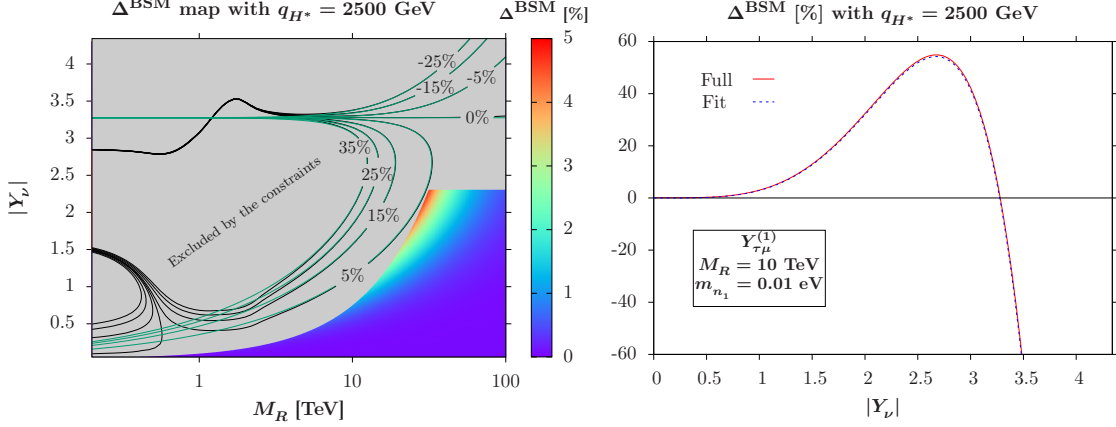


Figure 3. Left: Contour map of the heavy neutrino correction Δ^{BSM} to the triple Higgs coupling λ_{HHH} (in percent) as a function of the neutrino parameters M_R (in TeV) and $|Y_\nu|$ in the μ_X -parameterization. The Yukawa texture $Y_{\tau\mu}^{(1)}$ defined in eq.(4.4) is used and the off-shell Higgs boson momentum is fixed to $q_H^* = 2500$ GeV. The gray area is excluded by the constraints on the model. The green lines are the approximated contour lines using eq.(4.5) while the black lines correspond to the full calculation. Right: The heavy neutrino correction Δ^{BSM} (in percent) as a function of the Yukawa scaling parameter $|Y_\nu|$, in the μ_X -parameterization with the texture $Y_{\tau\mu}^{(1)}$. We have fixed the other input parameters for the neutrino sector as $M_R = 10$ TeV and $m_{n_1} = 0.01$ eV. The red (solid) curve corresponds to the full calculation, the blue (dashed) curve to the approximate result obtained with eq.(4.5).

To get an insight into the behavior of the contour lines in Fig. 3 (left) we display a one-dimensional plot of the neutrino correction Δ^{BSM} at a given $M_R = 10$ TeV, as a function of the Yukawa scaling factor $|Y_\nu|$, in Fig. 3 (right). The correction is negligible for low Yukawa scaling factors, then rises to a maximum at $\sim +60\%$ at $|Y_\nu| \simeq 2.5$ before dropping rapidly and eventually becoming negative for large Yukawa scaling factors.

From this behavior we devise the following approximate formula to reproduce Δ^{BSM} at $M_R > 3$ TeV,

$$\Delta_{\text{approx}}^{\text{BSM}} = \frac{(1 \text{ TeV})^2}{M_R^2} \left(8.45 \text{Tr}(Y_\nu Y_\nu^\dagger Y_\nu Y_\nu^\dagger) - 0.145 \text{Tr}(Y_\nu Y_\nu^\dagger Y_\nu Y_\nu^\dagger Y_\nu Y_\nu^\dagger) \right). \quad (4.5)$$

The numerical coefficients are found to be universal in term of the parameters of the model and only depend on the kinematics of the off-shell Higgs boson, for the case of the three textures of ref. [37] as well as for the case of a diagonal texture. The dependence of the numerical coefficients on the kinematics of the off-shell Higgs boson is expected, as when compared to the full calculation they would result from the loop functions depending on q_H^* , see Appendix B. It is expected that eq.(4.5) be valid for the whole class of textures introduced in Ref. [37]. At a given $M_R > 3$ TeV, the approximate formula in eq.(4.5) is driven at low $|Y_\nu|$ by the positive contribution and by the negative contribution at high $|Y_\nu|$, the latter falling

more rapidly than the positive increase at low $|Y_\nu|$. This reproduces the behavior seen in Fig. 3 (right) where the result of the fit is also displayed. We can also reproduce the contour lines for high M_R in Fig. 3 (left) as seen from the green contour lines coming from the fit, that agree to a very good extent with the full contour lines for $M_R > 3$ TeV.

The approximate formula in eq.(4.5) implies that the best way to maximize the neutrino effects on the triple Higgs coupling would be to maximize the ratio $\frac{\text{Tr}(Y_\nu Y_\nu^\dagger Y_\nu Y_\nu^\dagger)}{\text{Tr}(Y_\nu Y_\nu^\dagger Y_\nu Y_\nu^\dagger)}$. The Yukawa couplings being real and limited by perturbativity requirements, this leads to the choice of a diagonal texture, $Y_\nu \propto I_3$. This will be considered in the next sub-section, but with the condition of degenerate heavy neutrinos being relaxed. In such a way the constraints on the non-unitarity of the matrix \tilde{U}_{PMNS} are softened and the blue region of the Casas-Ibarra scan of Fig. 2, excluded by EWPO as well as by LFV observables, moves down.

4.3 Hierarchical heavy neutrinos

The analysis carried in the previous sub-section has lead us to consider a diagonal Yukawa matrix, $Y_\nu = |Y_\nu|I_3$. In order to reduce as much as possible the impact of unitarity constraints on η for the matrix \tilde{U}_{PMNS} , we chose hierarchical heavy neutrinos with $M_R = \text{diag}(M_{R_1}, M_{R_2}, M_{R_3})$ and we still work in the μ_X -parameterization. More specifically, for illustrative purpose within this class of parameters, we chose

$$M_{R_1} = 1.51M_R, \quad M_{R_2} = 3.59M_R, \quad M_{R_3} = M_R, \quad (4.6)$$

with M_R being a rescaling factor that is varied between 200 GeV and 20 TeV. This choice ensures that all the constraints of eq.(2.19) have the same impact on our study.

The result of the parameter scan in the $M_R - |Y_\nu|$ plane is displayed in Fig. 4. On the left-hand side, we display the map of Δ^{BSM} for an off-shell Higgs momentum $q_H^* = 500$ GeV. As already expected by the analysis in the simplified model of Ref. [26], the heavy neutrino corrections are negative, and they reach a minimum of $\sim -8\%$, close to the minimum that was obtained in the simplified model. The most interesting results are displayed in the right-hand side of Fig. 4, for $q_H^* = 2500$ GeV. The corrections can now reach a maximum of $\sim +30\%$, similar to what has been obtained in the case of a simplified model. The corrections are generically bigger in the ISS model than in the simplified model, but the constraints are also stronger, reducing the heavy neutrino corrections back to the maximum obtained in the simplified model. This also confirms in a realistic, renormalizable, low-scale seesaw model that heavy Majorana neutrinos can induce sizable deviation to the triple Higgs coupling.

As a further test of our approximate formula for the heavy neutrino corrections, the green lines in Fig. 4 are the approximate contour lines obtained using eq.(4.5) but rescaled with a common factor $\gamma = 0.51$. This type of rescaling was expected as now the heavy neutrino mass matrix is not proportional to the identity matrix anymore. Once again we obtain a very good approximation for $M_R > 3$ TeV, and in particular in the region allowed by the constraints. This approximate formula thus describes well the behavior of Δ^{BSM} in the allowed region of the parameter space, for $q_H^* = 2500$ GeV.

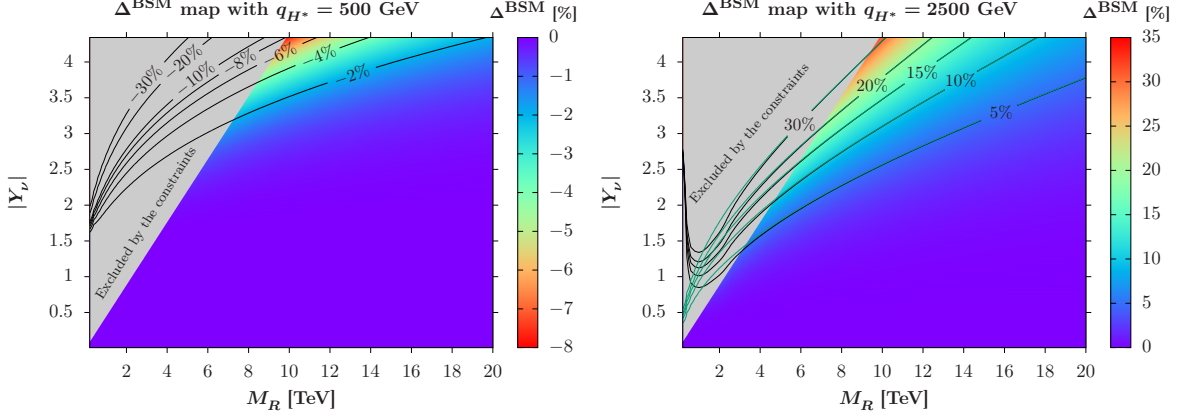


Figure 4. Contour map of the heavy neutrino correction Δ^{BSM} to the triple Higgs coupling λ_{HHH} (in percent) as a function of the neutrino parameters M_R (in TeV) and $|Y_\nu|$ in the μ_X -parameterization, using a diagonal Yukawa texture and a hierarchical heavy neutrino mass matrix with the parameters defined in eq.(4.6). The off-shell Higgs boson momentum is fixed to $q_H^* = 500$ GeV (left) and $q_H^* = 2500$ GeV (right). The gray area is excluded by the constraints on the model and the green lines on the right figure are the approximated contour lines using eq.(4.5) with a common rescaling factor 0.51, while the black lines correspond to the full calculation.

We end this section with a comparison with the currently expected sensitivity to the triple Higgs coupling at the HL-LHC and at the future planned colliders. The sensitivities to the SM triple Higgs coupling are defined by its measure extracted from the Higgs pair production yields. As stated for example in Refs. [55, 56], a precision of $\sim 50\%$ on the total cross section leads to a precision of $\sim 50\%$ on the SM triple Higgs coupling. The sensitivity for the HL-LHC follows from Ref. [31] (see also Ref. [57]), scaled by a factor of $1/\sqrt{2}$ to account for both ATLAS and CMS accumulated data, while the sensitivity for the future colliders follow from Refs. [32, 33]. For the FCC-hh we do the same as for the HL-LHC to account for both ATLAS and CMS accumulated data¹, as well as for the fact that the analysis in Ref. [33] is only done for one search channel; we expect the sensitivity to improve when more search channels are taken into account. We display in Fig. 5 the maximally allowed deviation Δ^{BSM} (in percent), in black solid line, as a function of the heavy neutrino rescaling factor M_R (in TeV). This is compared to the sensitivities to the SM prediction for λ_{HHH} in the case of the HL-LHC with an integrated luminosity of 3 ab^{-1} (dashed black line); the ILC with different center-of-mass energies \sqrt{s} and integrated luminosities \mathcal{L} , $\sqrt{s} = 500$ GeV and $\mathcal{L} = 4 \text{ ab}^{-1}$ (double dotted blue line), $\sqrt{s} = 1$ TeV and $\mathcal{L} = 2 \text{ ab}^{-1}$ (dotted purple line), $\sqrt{s} = 1$ TeV and $\mathcal{L} = 5 \text{ ab}^{-1}$ (long dash-dotted green line); and the case of the FCC-hh at 100 TeV and with

¹ It shall be mentioned that other analyses give more conservative prospects for the FCC-hh as well as for the HL-LHC, see for example Ref. [58]. However, new techniques in the meantime can be developed to help increasing the sensitivity, as well as a better analysis of possible search channels, see for example the case of the $4b$ final state [59].

Future colliders sensibility with $q_{H^*} = 2500$ GeV

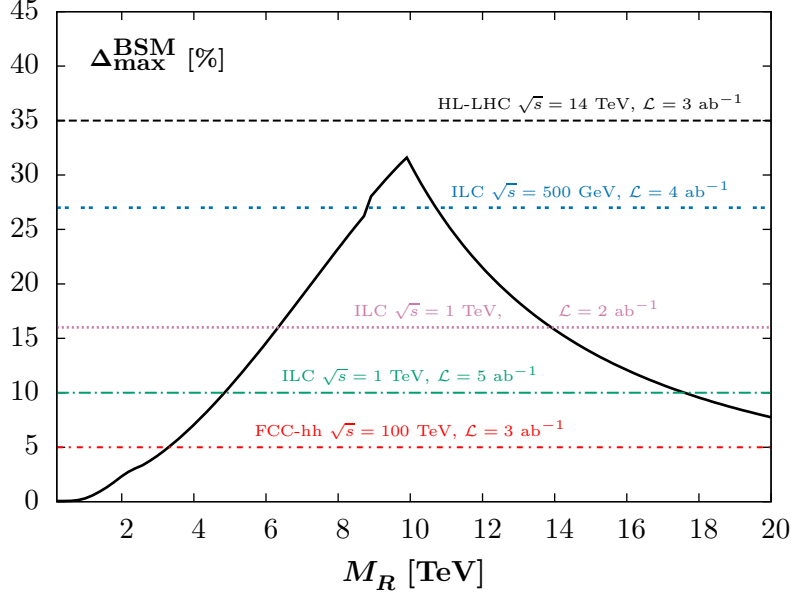


Figure 5. The maximally allowed deviation $\Delta_{\max}^{\text{BSM}}$ (in percent) as a function of the heavy neutrino mass parameter M_R (in TeV), compared to the currently expected sensitivities for the HL-LHC and the future ILC (with different integrated luminosities and center-of-mass energies \sqrt{s}) and FCC-hh colliders. The solid black line displays $\Delta_{\max}^{\text{BSM}}$, the dashed black line is the LHC-LHC sensitivity at 3 ab^{-1} , the double-dotted blue line is the ILC sensitivity at 4 ab^{-1} with $\sqrt{s} = 500$ GeV, the dotted line is the ILC sensitivity at 2 ab^{-1} with $\sqrt{s} = 1$ TeV, the green long dash-dotted line is the ILC sensitivity at 5 ab^{-1} with $\sqrt{s} = 1$ TeV, and the red dash-dotted line is the FCC-hh sensitivity at 3 ab^{-1} .

$\mathcal{L} = 3 \text{ ab}^{-1}$ (dash-dotted red line). While the currently foreseen sensitivity of the HL-LHC would not allow to resolve the effect of the heavy neutrinos, new analysis techniques or the other future colliders would clearly allow to test these heavy neutrino corrections.

More specifically, the ILC at a center-of-mass energy $\sqrt{s} = 500$ GeV could probe heavy neutrino masses in the range $8.5 < M_R < 10.5$ TeV, at 1 TeV with 5 ab^{-1} of data this extends to the range $5 < M_R < 17.5$ TeV. The FCC-hh collider could extend the analysis to a bigger range $3.3 < M_R < 20$ TeV. These are mass ranges that would be hard to probe otherwise, making the triple Higgs coupling a new, viable and attractive observable to test low-scale seesaw mechanisms.

5 Conclusions

We have investigated in this article the one-loop effects of heavy neutrinos on the triple Higgs coupling in the framework of an inverse seesaw model, that is a realistic, renormalizable

model accounting for the masses and mixings of the light neutrinos. After having presented the model and its constraints, both theoretical and experimental, in Section 2, we have given the technical details of the one-loop calculation in Section 3. We have presented in Section 4 our numerical investigation of the model. After having performed a scan in a Casas-Ibarra parameterization of the neutrino input parameters we have found that a μ_X -parameterization is more suitable to get the maximal effects on the triple Higgs coupling and we have obtained a deviation as high as $\sim +30\%$ for the class of parameters in which the 3×3 heavy neutrino mass matrix M_R is diagonal and hierarchical while the 3×3 neutrino Yukawa texture is proportional to the identity matrix. This confirms our expectations coming from the simplified model analysis, and establishes the triple Higgs coupling as a viable, new observable to probe heavy neutrino mass regimes that are hard to probe otherwise, as this deviation is at the current limit for the expected sensitivity at the HL-LHC but clearly visible at the ILC and at the FCC-hh. Heavy neutrinos can also give rise to new diagrams that contribute to the complete HH production cross section and need to be evaluated. We leave this for future projects.

Acknowledgments

We warmly thank Nadège Bernard for her logistic support during the last stage of the project. C.W. heartfully thanks the University of Tübingen for its hospitality during the final stages of this project. We also acknowledge the discussions with Juraj Streicher as well as with the participants of the *Focus Meeting on Collider Phenomenology*, organized at the IBS CTPU, Daejeon, South Korea. J.B. acknowledges the support from the Institutional Strategy of the University of Tübingen (DFG, ZUK 63) and from the DFG Grant JA 1954/1. C.W. receives financial support from the European Research Council under the European Union's Seventh Framework Programme (FP/2007-2013)/ERC Grant NuMass Agreement No. 617143 and partial support from the European Union's Horizon 2020 research and innovation programme under the Marie Skłodowska-Curie grant agreements No. 690575 and No. 674896. The Feynman diagrams of this article have been drawn with the program **JaxoDraw 2.0** [60, 61].

A Next order corrections to the μ_X -parameterization

Following the method of [62], we can diagonalize M_{ISS} by block to an arbitrary order in the seesaw expansion parameter $m_D M_R^{-1}$. This gives for the 3×3 light neutrino mass matrix

$$\begin{aligned}
M_{\text{light}} = & m_D M_R^{T-1} \mu_X M_R^{-1} m_D^T - \frac{1}{2} m_D M_R^{T-1} M_R^{*-1} m_D^\dagger m_D M_R^{T-1} \mu_X M_R^{-1} m_D^T \\
& - \frac{1}{2} m_D M_R^{T-1} \mu_X M_R^{-1} m_D^T m_D^* M_R^{\dagger-1} M_R^{-1} m_D^T + \text{o}(\|M_R^{-1} m_D\|^4) \times \mu_X,
\end{aligned} \tag{A.1}$$

in agreement with previous results [63]. This can be written in a symmetric form

$$M_{\text{light}} = m_D M_R^{T-1} \left(\mathbf{1} - \frac{1}{2} M_R^{*-1} m_D^\dagger m_D M_R^{T-1} \right) \mu_X \left(\mathbf{1} - \frac{1}{2} M_R^{-1} m_D^T m_D^* M_R^{\dagger-1} \right) M_R^{-1} m_D^T + o(\|M_R^{-1} m_D\|^4) \times \mu_X. \quad (\text{A.2})$$

If m_D is invertible, we can then express μ_X as a function of M_{light} and the other blocks of M_{ISS} ,

$$\mu_X \simeq \left(\mathbf{1} - \frac{1}{2} M_R^{*-1} m_D^\dagger m_D M_R^{T-1} \right)^{-1} M_R^T m_D^{-1} M_{\text{light}} m_D^{T-1} M_R \left(\mathbf{1} - \frac{1}{2} M_R^{-1} m_D^T m_D^* M_R^{\dagger-1} \right)^{-1}. \quad (\text{A.3})$$

The light neutrino mass matrix is diagonalized by using the unitary PMNS matrix. Using eq.(2.7) to rewrite M_{light} in eq.(A.3), we get a formula for the μ_X -parameterization that includes the effect of sub-leading terms in the seesaw expansion,

$$\mu_X \simeq \left(\mathbf{1} - \frac{1}{2} M_R^{*-1} m_D^\dagger m_D M_R^{T-1} \right)^{-1} M_R^T m_D^{-1} U_{\text{PMNS}}^* m_\nu U_{\text{PMNS}}^\dagger m_D^{T-1} M_R \times \left(\mathbf{1} - \frac{1}{2} M_R^{-1} m_D^T m_D^* M_R^{\dagger-1} \right)^{-1}. \quad (\text{A.4})$$

It is easy to see that if we were to consider only the leading order term in the seesaw expansion, we would recover eq.(45) from [37].

Interestingly, our results would not be modified by the addition of an extra mass term $\mu_R \nu_R^C \nu_R$. The neutrino mass matrix would then be

$$M = \begin{pmatrix} 0 & m_D & 0 \\ m_D^T & \mu_R & M_R \\ 0 & M_R^T & \mu_X \end{pmatrix}, \quad (\text{A.5})$$

where taking $\|\mu_R\| \ll \|m_D\|, \|M_R\|$ corresponds to the inverse seesaw limit while taking $\|\mu_R\| \geq \|M_R\|$ leads to the extended seesaw limit. In both cases, the next order corrections to M_{light} are given by eq.(A.1) in the limit where $\|\mu_X M_R^{-1} \mu_R\| \ll \|M_R\|$. Thus, eq.(2.12) would remain unchanged.

B Analytic expressions of the new ISS contributions

We give in this appendix all the analytic formulae of the new ISS contributions involved in the calculation of the renormalized one-loop triple Higgs coupling presented in Section 3. The SM contributions, denoted with a SM, can be found in ref. [46] and will not be reproduced in this appendix.

B.1 Counter-terms

By convention all loop integrals in this sub-section are to be understood as their real part only. We use the conventions of `LoopTools` 2.13 [49, 52, 53] for the scalar integrals and the tensor coefficients.

$$\begin{aligned} \delta M_W^2 = \delta M_W^2|_{\text{SM}} - \frac{\alpha}{4\pi s_W^2} \sum_{i=1}^3 \sum_{j=1}^9 |B_{ij}|^2 \Big(& A_0(m_{n_j}^2) + m_{\ell_i}^2 B_0(M_W^2, m_{\ell_i}^2, m_{n_j}^2) \\ & - 2B_{00}(M_W^2, m_{\ell_i}^2, m_{n_j}^2) + M_W^2 B_1(M_W^2, m_{\ell_i}^2, m_{n_j}^2) \Big) \end{aligned} \quad (\text{B.1})$$

$$\begin{aligned} \delta M_Z^2 = \delta M_Z^2|_{\text{SM}} - \frac{3\alpha}{48\pi c_W^2 s_W^2} \sum_{j=1}^9 \sum_{k=1}^9 \Big(& (C_{jk} C_{kj}^* + C_{jk}^* C_{kj}) m_{n_j} m_{n_k} B_0(M_Z^2, m_{n_j}^2, m_{n_k}^2) \\ & + (C_{jk} C_{kj} + C_{jk}^* C_{kj}^*) \Big(A_0(m_{n_k}^2) + m_{n_j}^2 B_0(M_Z^2, m_{n_j}^2, m_{n_k}^2) - 2B_{00}(M_Z^2, m_{n_j}^2, m_{n_k}^2) \\ & + M_Z^2 B_1(M_Z^2, m_{n_j}^2, m_{n_k}^2) \Big) \Big) \end{aligned} \quad (\text{B.2})$$

$$\delta t_H = \delta t_H|_{\text{SM}} - \frac{\sqrt{2\pi\alpha}}{8\pi^2 M_W s_W} \sum_{j=1}^9 m_{n_j}^2 \text{Re}(C_{jj}) A_0(m_{n_j}^2) \quad (\text{B.3})$$

B.2 One-loop un-renormalized self energy Σ_{HH} and vertex $\lambda_{HHH}^{(1)}$

The self-energy enters in the calculation of the field renormalization as well as the Higgs mass M_H counter-term. In the one-loop un-renormalized triple Higgs coupling, q is the momentum of the off-shell Higgs boson splitting into two Higgs bosons, $H^*(q) \rightarrow HH$.

$$\begin{aligned} \Sigma_{HH}(p^2) = \Sigma_{HH}^{\text{SM}}(p^2) - \frac{\alpha}{16\pi M_W^2 s_W^2} \sum_{j=1}^9 \sum_{k=1}^9 \Big(& (C_{jk} C_{kj} + C_{jk}^* C_{kj}^*) m_{n_j}^2 \Big(A_0(m_{n_k}^2) \\ & + p^2 B_1(p^2, m_{n_j}^2, m_{n_k}^2) + m_{n_j}^2 B_0(p^2, m_{n_j}^2, m_{n_k}^2) \Big) + (C_{jk} C_{kj} + C_{jk}^* C_{kj}^*) m_{n_k}^2 \Big(A_0(m_{n_k}^2) \\ & + p^2 B_1(p^2, m_{n_j}^2, m_{n_k}^2) + 3m_{n_j}^2 B_0(p^2, m_{n_j}^2, m_{n_k}^2) \Big) + (C_{kj} C_{jk}^* + C_{jk} C_{kj}^*) m_{n_j} m_{n_k} \\ & \Big(2A_0(m_{n_k}^2) + 2p^2 B_1(p^2, m_{n_j}^2, m_{n_k}^2) + 3m_{n_j}^2 B_0(p^2, m_{n_j}^2, m_{n_k}^2) \Big) \\ & + (C_{kj} C_{jk}^* + C_{jk} C_{kj}^*) m_{n_j} m_{n_k}^3 B_0(p^2, m_{n_j}^2, m_{n_k}^2) \Big) \end{aligned} \quad (\text{B.4})$$

$$\begin{aligned}
\lambda_{HHH}^{(1)}(q) = & \lambda_{HHH}^{(1),\text{SM}}(q) - \frac{\alpha\sqrt{4\pi\alpha}}{32\pi M_W^3 s_W^3} \sum_{j=1}^9 \sum_{k=1}^9 \sum_{l=1}^9 \left[\left(C_{jk} C_{kl} C_{lj} + C_{jk}^* C_{kl}^* C_{lj}^* \right) \right. \\
& \left(m_{n_j}^2 m_{n_k}^2 \left(4B_0 + 4M_H^2 C_2 + q^2 (C_0 + 4C_1 + C_2) + 4m_{n_j}^2 C_0 \right) \right. \\
& + m_{n_l}^2 m_{n_k}^2 \left(4B_0 + 2M_H^2 C_2 + q^2 (3C_1 + C_2) \right) + m_{n_l}^2 m_{n_j}^2 \left(4B_0 + \right. \\
& \left. 4(m_{n_j}^2 + 2m_{n_k}^2) C_0 + 2M_H^2 C_2 + q^2 (C_0 + 5C_1 + 2C_2) \right) \left. \right) + \\
& m_{n_j} m_{n_l} \left(C_{jk} C_{kl} C_{jl} + C_{jk}^* C_{kl}^* C_{jl}^* \right) \left(m_{n_l}^2 \left(2B_0 + q^2 (2C_1 + C_2) \right) + \right. \\
& m_{n_k}^2 \left(8B_0 + 6M_H^2 C_2 + q^2 (C_0 + 7C_1 + 2C_2) + 2m_{n_l}^2 C_0 \right) + \\
& m_{n_j}^2 \left(2B_0 + 2M_H^2 C_2 + q^2 (C_0 + 3C_1 + C_2) + 2(5m_{n_k}^2 + m_{n_j}^2 + m_{n_l}^2) C_0 \right) \left. \right) + \\
& m_{n_k} m_{n_l} \left(C_{jk} C_{lk} C_{lj} + C_{jk}^* C_{lk}^* C_{lj}^* \right) \left(m_{n_k}^2 \left(2B_0 + 2M_H^2 C_2 + q^2 C_1 \right) + \right. \\
& m_{n_l}^2 \left(2B_0 + q^2 (2C_1 + C_2) \right) + m_{n_j}^2 \left(8B_0 + 6M_H^2 C_2 + q^2 (2C_0 + 9C_1 + 3C_2) + \right. \\
& \left. 4(2m_{n_j}^2 + m_{n_k}^2 + m_{n_l}^2) C_0 \right) \left. \right) + \\
& m_{n_j} m_{n_k} \left(C_{jk} C_{lk} C_{jl} + C_{jk}^* C_{lk}^* C_{jl}^* \right) \left(m_{n_l}^2 \left(8B_0 + 4M_H^2 C_2 + q^2 (C_0 + 8C_1 + 3C_2) \right) + \right. \\
& m_{n_k}^2 \left(2B_0 + 2M_H^2 C_2 + q^2 C_1 + 2m_{n_l}^2 C_0 \right) + m_{n_j}^2 \left(2B_0 + 2M_H^2 C_2 + \right. \\
& \left. q^2 (C_0 + 3C_1 + C_2) + 2C_0 (m_{n_j}^2 + m_{n_k}^2 + 5m_{n_l}^2) \right) \left. \right) \left. \right] \quad (\text{B.5})
\end{aligned}$$

In the expression of the un-renormalized vertex $\lambda_{HHH}^{(1)}$ we have used the following abbreviations,

$$\begin{aligned}
B_0 &\equiv B_0(M_H^2, m_{n_k}^2, m_{n_l}^2) , \\
C_0 &\equiv C_0(q^2, M_H^2, M_H^2, m_{n_j}^2, m_{n_k}^2, m_{n_l}^2) , \\
C_{1/2} &\equiv C_{1/2}(q^2, M_H^2, M_H^2, m_{n_j}^2, m_{n_k}^2, m_{n_l}^2) . \quad (\text{B.6})
\end{aligned}$$

References

- [1] ATLAS collaboration, G. Aad et al., *Observation of a new particle in the search for the Standard Model Higgs boson with the ATLAS detector at the LHC*, *Phys.Lett.* **B716** (2012) 1–29, [[1207.7214](#)].
- [2] CMS collaboration, S. Chatrchyan et al., *Observation of a new boson at a mass of 125 GeV with the CMS experiment at the LHC*, *Phys.Lett.* **B716** (2012) 30–61, [[1207.7235](#)].

- [3] P. W. Higgs, *Broken symmetries, massless particles and gauge fields*, [*Phys.Lett.* **12** \(1964\) 132–133](#).
- [4] F. Englert and R. Brout, *Broken Symmetry and the Mass of Gauge Vector Mesons*, [*Phys.Rev.Lett.* **13** \(1964\) 321–323](#).
- [5] P. W. Higgs, *Broken Symmetries and the Masses of Gauge Bosons*, [*Phys.Rev.Lett.* **13** \(1964\) 508–509](#).
- [6] G. Guralnik, C. Hagen and T. Kibble, *Global Conservation Laws and Massless Particles*, [*Phys.Rev.Lett.* **13** \(1964\) 585–587](#).
- [7] J. M. Cornwall, D. N. Levin and G. Tiktopoulos, *Uniqueness of spontaneously broken gauge theories*, [*Phys. Rev. Lett.* **30** \(1973\) 1268–1270](#).
- [8] C. H. Llewellyn Smith, *High-Energy Behavior and Gauge Symmetry*, [*Phys. Lett.* **B46** \(1973\) 233–236](#).
- [9] SUPER-KAMIOKANDE collaboration, Y. Fukuda et al., *Evidence for oscillation of atmospheric neutrinos*, [*Phys. Rev. Lett.* **81** \(1998\) 1562–1567](#), [[hep-ex/9807003](#)].
- [10] P. Minkowski, $\mu \rightarrow e\gamma$ at a Rate of One Out of 10^9 Muon Decays?, [*Phys. Lett.* **B67** \(1977\) 421–428](#).
- [11] P. Ramond, *The Family Group in Grand Unified Theories*, in *International Symposium on Fundamentals of Quantum Theory and Quantum Field Theory Palm Coast, Florida, February 25-March 2, 1979*, pp. 265–280, 1979. [hep-ph/9809459](#).
- [12] M. Gell-Mann, P. Ramond and R. Slansky, *Complex Spinors and Unified Theories*, *Conf. Proc.* **C790927** (1979) 315–321, [[1306.4669](#)].
- [13] T. Yanagida, *Horizontal Symmetry and Masses of Neutrinos*, *Conf. Proc.* **C7902131** (1979) 95–99.
- [14] R. N. Mohapatra and G. Senjanovic, *Neutrino Mass and Spontaneous Parity Violation*, [*Phys. Rev. Lett.* **44** \(1980\) 912](#).
- [15] J. Schechter and J. W. F. Valle, *Neutrino Masses in $SU(2) \times U(1)$ Theories*, [*Phys. Rev.* **D22** \(1980\) 2227](#).
- [16] J. Schechter and J. W. F. Valle, *Neutrino Decay and Spontaneous Violation of Lepton Number*, [*Phys. Rev.* **D25** \(1982\) 774](#).
- [17] R. N. Mohapatra, *Mechanism for Understanding Small Neutrino Mass in Superstring Theories*, [*Phys. Rev. Lett.* **56** \(1986\) 561–563](#).
- [18] R. N. Mohapatra and J. W. F. Valle, *Neutrino Mass and Baryon Number Nonconservation in Superstring Models*, [*Phys. Rev.* **D34** \(1986\) 1642](#).
- [19] J. Bernab  , A. Santamaria, J. Vidal, A. Mendez and J. W. F. Valle, *Lepton Flavor Nonconservation at High-Energies in a Superstring Inspired Standard Model*, [*Phys. Lett.* **B187** \(1987\) 303](#).
- [20] A. Pilaftsis, *Radiatively induced neutrino masses and large Higgs neutrino couplings in the standard model with Majorana fields*, [*Z. Phys.* **C55** \(1992\) 275–282](#), [[hep-ph/9901206](#)].

- [21] A. Ilakovac and A. Pilaftsis, *Flavor violating charged lepton decays in seesaw-type models*, *Nucl. Phys.* **B437** (1995) 491, [[hep-ph/9403398](#)].
- [22] E. K. Akhmedov, M. Lindner, E. Schnapka and J. W. F. Valle, *Left-right symmetry breaking in NJL approach*, *Phys. Lett.* **B368** (1996) 270–280, [[hep-ph/9507275](#)].
- [23] E. K. Akhmedov, M. Lindner, E. Schnapka and J. W. F. Valle, *Dynamical left-right symmetry breaking*, *Phys. Rev.* **D53** (1996) 2752–2780, [[hep-ph/9509255](#)].
- [24] S. M. Barr, *A Different seesaw formula for neutrino masses*, *Phys. Rev. Lett.* **92** (2004) 101601, [[hep-ph/0309152](#)].
- [25] M. Malinský, J. C. Romão and J. W. F. Valle, *Novel supersymmetric $SO(10)$ seesaw mechanism*, *Phys. Rev. Lett.* **95** (2005) 161801, [[hep-ph/0506296](#)].
- [26] J. Baglio and C. Weiland, *Heavy neutrino impact on the triple Higgs coupling*, *Phys. Rev.* **D94** (2016) 013002, [[1603.00879](#)].
- [27] H. Baer, T. Barklow, K. Fujii, Y. Gao, A. Hoang, S. Kanemura et al., *The International Linear Collider Technical Design Report - Volume 2: Physics*, [1306.6352](#).
- [28] N. Arkani-Hamed, T. Han, M. Mangano and L.-T. Wang, *Physics Opportunities of a 100 TeV Proton-Proton Collider*, *Phys. Rept.* **652** (2016) 1–49, [[1511.06495](#)].
- [29] J. Baglio, A. Djouadi and J. Quevillon, *Prospects for Higgs physics at energies up to 100 TeV*, *Rep. Prog. Phys.* **79** (2016) 116201, [[1511.07853](#)].
- [30] R. Contino et al., *Physics at a 100 TeV pp collider: Higgs and EW symmetry breaking studies*, [1606.09408](#).
- [31] CMS collaboration, V. Khachatryan et al., *Higgs pair production at the High Luminosity LHC*, Tech. Rep. CMS-PAS-FTR-15-002, CERN, 2015.
- [32] K. Fujii et al., *Physics Case for the International Linear Collider*, [1506.05992](#).
- [33] H.-J. He, J. Ren and W. Yao, *Probing new physics of cubic Higgs boson interaction via Higgs pair production at hadron colliders*, *Phys. Rev.* **D93** (2016) 015003, [[1506.03302](#)].
- [34] B. Pontecorvo, *Mesonium and antimesonium*, *Zh. Eksp. Teor. Fiz.* **33** (1957) 549–551.
- [35] Z. Maki, M. Nakagawa and S. Sakata, *Remarks on the unified model of elementary particles*, *Prog. Theor. Phys.* **28** (1962) 870–880.
- [36] J. A. Casas and A. Ibarra, *Oscillating neutrinos and $\mu \rightarrow e, \gamma$* , *Nucl. Phys. B* **618** (2001) 171–204, [[hep-ph/0103065](#)].
- [37] E. Arganda, M. Herrero, X. Marcano and C. Weiland, *Imprints of massive inverse seesaw model neutrinos in lepton flavor violating Higgs boson decays*, *Phys.Rev.* **D91** (2015) 015001, [[1405.4300](#)].
- [38] I. Esteban, M. C. Gonzalez-Garcia, M. Maltoni, I. Martinez-Soler and T. Schwetz, *Updated fit to three neutrino mixing: exploring the accelerator-reactor complementarity*, [1611.01514](#).
- [39] PLANCK collaboration, P. A. R. Ade et al., *Planck 2015 results. XIII. Cosmological parameters*, *Astron. Astrophys.* **594** (2016) A13, [[1502.01589](#)].
- [40] E. Fernandez-Martinez, J. Hernandez-Garcia and J. Lopez-Pavon, *Global constraints on heavy neutrino mixing*, *JHEP* **08** (2016) 033, [[1605.08774](#)].

- [41] MEG collaboration, A. M. Baldini et al., *Search for the lepton flavour violating decay $\mu^+ \rightarrow e^+ \gamma$ with the full dataset of the MEG experiment*, *Eur. Phys. J. C* **76** (2016) 434, [[1605.05081](#)].
- [42] BABAR COLLABORATION collaboration, B. Aubert et al., *Searches for lepton flavor violation in the decays $\tau^\pm \rightarrow e^\pm \gamma$ and $\tau^\pm \rightarrow \mu^\pm \gamma$* , *Phys. Rev. Lett.* **104** (2010) 021802, [[0908.2381](#)].
- [43] SINDRUM COLLABORATION collaboration, U. Bellgardt et al., *Search for the decay $\mu^+ \rightarrow e^+ e^+ e^-$* , *Nucl. Phys. B* **299** (1988) 1.
- [44] K. Hayasaka, K. Inami, Y. Miyazaki, K. Arinstein, V. Aulchenko et al., *Search for lepton flavor violating τ decays into three leptons with 719 million produced $\tau^+ \tau^-$ pairs*, *Phys. Lett. B* **687** (2010) 139–143, [[1001.3221](#)].
- [45] A. Atre, T. Han, S. Pascoli and B. Zhang, *The Search for Heavy Majorana Neutrinos*, *JHEP* **05** (2009) 030, [[0901.3589](#)].
- [46] A. Denner, *Techniques for calculation of electroweak radiative corrections at the one loop level and results for W physics at LEP-200*, *Fortsch. Phys.* **41** (1993) 307–420, [[0709.1075](#)].
- [47] D. T. Nhung, M. Mühlleitner, J. Streicher and K. Walz, *Higher Order Corrections to the Trilinear Higgs Self-Couplings in the Real NMSSM*, *JHEP* **11** (2013) 181, [[1306.3926](#)].
- [48] T. Hahn, *Generating Feynman diagrams and amplitudes with FeynArts 3*, *Comput. Phys. Commun.* **140** (2001) 418–431, [[hep-ph/0012260](#)].
- [49] T. Hahn and M. Perez-Victoria, *Automatized one loop calculations in four-dimensions and D-dimensions*, *Comput. Phys. Commun.* **118** (1999) 153–165, [[hep-ph/9807565](#)].
- [50] G. 't Hooft and M. J. G. Veltman, *Scalar One Loop Integrals*, *Nucl. Phys. B* **153** (1979) 365–401.
- [51] G. Passarino and M. J. G. Veltman, *One Loop Corrections for $e^+ e^-$ Annihilation Into $\mu^+ \mu^-$ in the Weinberg Model*, *Nucl. Phys. B* **160** (1979) 151.
- [52] G. J. van Oldenborgh, *FF: A Package to evaluate one loop Feynman diagrams*, *Comput. Phys. Commun.* **66** (1991) 1–15.
- [53] T. Hahn and M. Rauch, *News from FormCalc and LoopTools*, *Nucl. Phys. Proc. Suppl.* **157** (2006) 236–240, [[hep-ph/0601248](#)].
- [54] PARTICLE DATA GROUP collaboration, C. Patrignani et al., *Review of Particle Physics*, *Chin. Phys.* **C40** (2016) 100001.
- [55] J. Baglio, A. Djouadi, R. Gröber, M. M. Mühlleitner, J. Quevillon and M. Spira, *The measurement of the Higgs self-coupling at the LHC: theoretical status*, *JHEP* **04** (2013) 151, [[1212.5581](#)].
- [56] R. Frederix, S. Frixione, V. Hirschi, F. Maltoni, O. Mattelaer, P. Torrielli et al., *Higgs pair production at the LHC with NLO and parton-shower effects*, *Phys. Lett. B* **732** (2014) 142–149, [[1401.7340](#)].
- [57] P. Campana, M. Klute and P. Wells, *Physics Goals and Experimental Challenges of the Proton-Proton High-Luminosity Operation of the LHC*, *Ann. Rev. Nucl. Part. Sci.* **66** (2016) 273–295, [[1603.09549](#)].
- [58] A. Azatov, R. Contino, G. Panico and M. Son, *Effective field theory analysis of double Higgs boson production via gluon fusion*, *Phys. Rev. D* **92** (2015) 035001, [[1502.00539](#)].

- [59] J. K. Behr, D. Bortoletto, J. A. Frost, N. P. Hartland, C. Issever and J. Rojo, *Boosting Higgs pair production in the $b\bar{b}b\bar{b}$ final state with multivariate techniques*, *Eur. Phys. J.* **C76** (2016) 386, [[1512.08928](#)].
- [60] D. Binosi and L. Theussl, *JaxoDraw: A Graphical user interface for drawing Feynman diagrams*, *Comput. Phys. Commun.* **161** (2004) 76–86, [[hep-ph/0309015](#)].
- [61] D. Binosi, J. Collins, C. Kaufhold and L. Theussl, *JaxoDraw: A Graphical user interface for drawing Feynman diagrams. Version 2.0 release notes*, *Comput. Phys. Commun.* **180** (2009) 1709–1715, [[0811.4113](#)].
- [62] W. Grimus and L. Lavoura, *The Seesaw mechanism at arbitrary order: Disentangling the small scale from the large scale*, *JHEP* **11** (2000) 042, [[hep-ph/0008179](#)].
- [63] H. Hettmansperger, M. Lindner and W. Rodejohann, *Phenomenological Consequences of sub-leading Terms in See-Saw Formulas*, *JHEP* **1104** (2011) 123, [[1102.3432](#)].